MZB1 promotes the secretion of J-chain–containing dimeric IgA and is critical for the suppression of gut inflammation

Ermeng Xiong[a,1], Yingqian Li[a,1], Qing Min[a,1], Chaoqun Cui[a], Jun Liu[a], Rongjian Hong[a], Nannan Lai[a], Ying Wang[a], Jiping Sun[a], Ryohtaroh Matsumoto[b], Daisuke Takahashi[b], Koji Hase[b], Reiko Shinkura[c], Takeshi Tsubata[d], and Ji-Yang Wang[a,d,2]

[a]Department of Immunology, School of Basic Medical Sciences, Fudan University, 200032 Shanghai, China; [b]Division of Biochemistry, Faculty of Pharmacy, Keio University, 105-8512 Tokyo, Japan; [c]Laboratory of Immunology and Infection Control, Institute of Quantitative Biosciences, University of Tokyo, 113-0032 Tokyo, Japan; and [d]Department of Immunology, Medical Research Institute, Tokyo Medical and Dental University, 113-8510 Tokyo, Japan

IgA is the most abundantly produced antibody in the body and plays a crucial role in gut homeostasis and mucosal immunity. IgA forms a dimer that covalently associates with the joining (J) chain, which is essential for IgA transport into the mucosa. Here, we demonstrate that the marginal zone B and B-1 cell-specific protein (MZB1) interacts with IgA through the α-heavy-chain tailpiece dependent on the penultimate cysteine residue and prevents the intracellular degradation of α-light-chain complexes. Moreover, MZB1 promotes J-chain binding to IgA and the secretion of dimeric IgA. MZB1-deficient mice are impaired in secreting large amounts of IgA into the gut in response to acute inflammation and develop severe colitis. Oral administration of a monoclonal IgA significantly ameliorated the colitis, accompanied by normalization of the gut microbiota composition. The present study identifies a molecular chaperone that promotes J-chain binding to IgA and reveals an important mechanism that controls the quantity, quality, and function of IgA.

immunoglobulin A | J chain | heavy chain tailpiece | molecular chaperone | gut homeostasis

IgA is the most abundant antibody (Ab) produced in mammals (in humans, >5 g/d), an amount greater than all of the other Ab isotypes combined (1–4). IgA is secreted across mucous membranes (5, 6). While human selective IgA deficiency (SIgAD) was long considered asymptomatic (7), detailed studies revealed that SIgAD is associated with increased incidence of respiratory infections, allergy, autoimmunity, and intestinal disorders such as inflammatory bowel disease (8–10). Murine models of IgA deficiency in the gut, such as mice lacking the joining (J) chain, poly-Ig receptor (pIgR), or activation-induced cytidine deaminase, confirmed that IgA is important in intestinal immune protection (11–13). The primary function of mucosal IgA is to shape the microbiome and regulate intestinal homeostasis (4, 14, 15). Unlike IgG and IgM, IgA does not activate the classical complement pathway and exerts an anti-inflammatory effect (16).

IgA can be found in both monomeric and dimeric forms (17). There are considerable differences in the levels of monomeric and dimeric IgA in serum and secretions among different species. Serum IgA is primarily represented by monomeric form in humans with two heavy chains (HCs) and two light chains (LCs), whereas mucosal IgA predominantly consists of dimers, comprising two IgA monomers linked to one molecule of the J chain (18). IgA secretion at mucosal surfaces is mediated by the pIgR expressed on the basolateral surface of intestinal epithelial cells, which binds to IgA, dependent on the presence of the J chain (19). After the transport, the extracellular domain of pIgR, known as the secretory component (SC), is cleaved off the epithelial cell and remains bound to IgA. The complex of dimeric IgA, the J chain, and SC is called secretory IgA (sIgA) (20). In contrast to the gut, in blood, IgG is the predominant Ab isotype and the prominent Ab produced during a T cell-dependent humoral response. Structurally, IgG is different from IgA and IgM in that it does not multimerize

(21). The secretory forms of both α- and μ-HC possess an 18-amino-acid-long extension to the C-terminal constant domain, termed the secretory tailpiece (22, 23). The tailpiece contains a preterminal cysteine residue, which is the site for the covalent attachment of the J chain to IgA and IgM polymers (24, 25) and is necessary for the assembly of dimeric IgA and polymeric IgM (26). Quality control of sIgA and IgM assembly in the endoplasmic reticulum (ER) requires the tailpiece (27).

MZB1 (marginal zone B and B-1 cell-specific protein) is a B cell-specific and ER-localized protein (28). It is most abundantly expressed in marginal zone (MZ) B and B-1 cells (29) and up-regulated during B cell differentiation into plasma cells (30). Earlier studies revealed that MZB1 is a cochaperone of BiP and GRP94 that enables proper folding of Ig μHC and LC and efficient IgM secretion (28, 30). Using siRNA-mediated knockdown of MZB1, Flach et al. (29) reported that MZB1 regulated Ca^{2+} homeostasis and IgM production in primary B cells. More recently, Rosenbaum et al. (31) generated MZB1-deficient mice and found that MZB1 is a GRP94 cochaperone that promotes IgM biosynthesis. These studies have revealed a role for MZB1 in the assembly and/or biosynthesis of IgM. However, whether MZB1 is involved in the synthesis or secretion of IgA and IgG remains unknown.

Significance

IgA is the most abundantly produced antibody in the body (in humans, >5 g/d) and plays a crucial role in mucosal immunity. IgA forms a dimer that covalently associates with the joining (J) chain, which is essential for IgA transport into the gut. We show that MZB1 is required for the secretion of IgA, but not IgG, by antibody-secreting plasma cells. MZB1 mediates the stabilization of Igα heavy-chain–light-chain complexes and, more importantly, promotes J-chain binding to IgA. Mice lacking MZB1 are impaired in secreting large amounts of IgA into the gut in response to acute inflammatory stimuli and develop severe colitis. The present study reveals an important mechanism that controls the quantity, quality, and function of IgA.

In the present study, we show that MZB1 is required for efficient secretion of IgA, but not IgG, both in vitro and in vivo. MZB1 physically interacts with the αHC tailpiece (αtp), dependent on the penultimate cysteine residue, and prevents the degradation of intracellular αHC–LC (αL) complexes. Moreover, MZB1 promotes J-chain binding to IgA and the secretion of dimeric IgA. MZB1-deficient mice are impaired in secreting large amounts of IgA into the gut in response to acute inflammatory stimuli. In addition, the mutant mice suffer from aggravated dextran sodium sulfate (DSS)-induced colitis, accompanied by microbiota dysbiosis. Administration of a monoclonal IgA represses the sensitivity to DSS-induced colitis in MZB1-deficient mice and concomitantly normalizes the microbiota composition in the gut. Our results identify MZB1 as a molecular chaperone required for efficient secretion of J-chain–containing dimeric IgA and suppression of gut inflammation.

Results

MZB1 Is Required for Efficient Secretion of IgA and IgM, but Not IgG, in Vitro and in Vivo.

$Mzb1$ is preferentially expressed in B cells, as revealed by our microarray analysis of gene expression in various immune and nonimmune cells (*SI Appendix*, Fig. S1*A*). To explore the physiological role of MZB1 in B cells, we generated $Mzb1^{-/-}$ mice (*SI Appendix*, Fig. S1 *B–D*). $Mzb1^{-/-}$ mice developed and bred normally without apparent abnormalities. B cell development, maturation, and activation were also not affected (*SI Appendix*, Fig. S2 *A–E*). However, serum IgA levels

were dramatically decreased in $Mzb1^{-/-}$ mice compared with $Mzb1^{+/+}$ mice (Fig. 1*A*). In addition, IgM levels were moderately but statistically significantly reduced in $Mzb1^{-/-}$ mice, in agreement with studies showing that MZB1 is involved in IgM biosynthesis (28, 30). In contrast, the levels of all four IgG subclasses (IgG_1, IgG_{2b}, IgG_{2c}, and IgG_3) in the serum were not different between $Mzb1^{+/+}$ and $Mzb1^{-/-}$ mice (Fig. 1*A*). These results indicate that MZB1 specifically regulated the production of IgA, and to a lesser extent IgM, but not IgG.

The reduced IgA levels could be due to impaired class switch recombination (CSR) to IgA, the generation of IgA plasma cells, or the secretion of IgA by plasma cells. To distinguish these possibilities, we first cultured $Mzb1^{+/+}$ and $Mzb1^{-/-}$ B cells in medium alone (Ctrl) or in the presence of recombinant CD40 ligand, IL-4, dextran-conjugated α-IgD, and TGFβ (CIDT) for 3 d and analyzed the frequency of IgA^+ cells (32). As shown in Fig. 1*B*, CIDT induced a similar proportion of the IgA^+ cells among $Mzb1^{+/+}$ and $Mzb1^{-/-}$ B cells. In addition, stimulation of $Mzb1^{+/+}$ and $Mzb1^{-/-}$ B cells with CD40 ligand + IL-4 (CI) induced a similar percentage of the IgG_1^+ cells (Fig. 1*C*). These results demonstrate that $Mzb1^{-/-}$ B cells have normal CSR to IgA and IgG_1. We next stimulated spleen B cells with lipopolysaccharide (LPS), CIDT, or CI to induce B cell differentiation into IgM-, IgA-, or IgG-producing plasma cells, respectively. As shown in Fig. 1 *D* and *E*, each of these stimuli induced a similar proportion of $B220^{dull}CD138^+$ plasma cells among $Mzb1^{+/+}$ and $Mzb1^{-/-}$ B cells. To directly prove that the
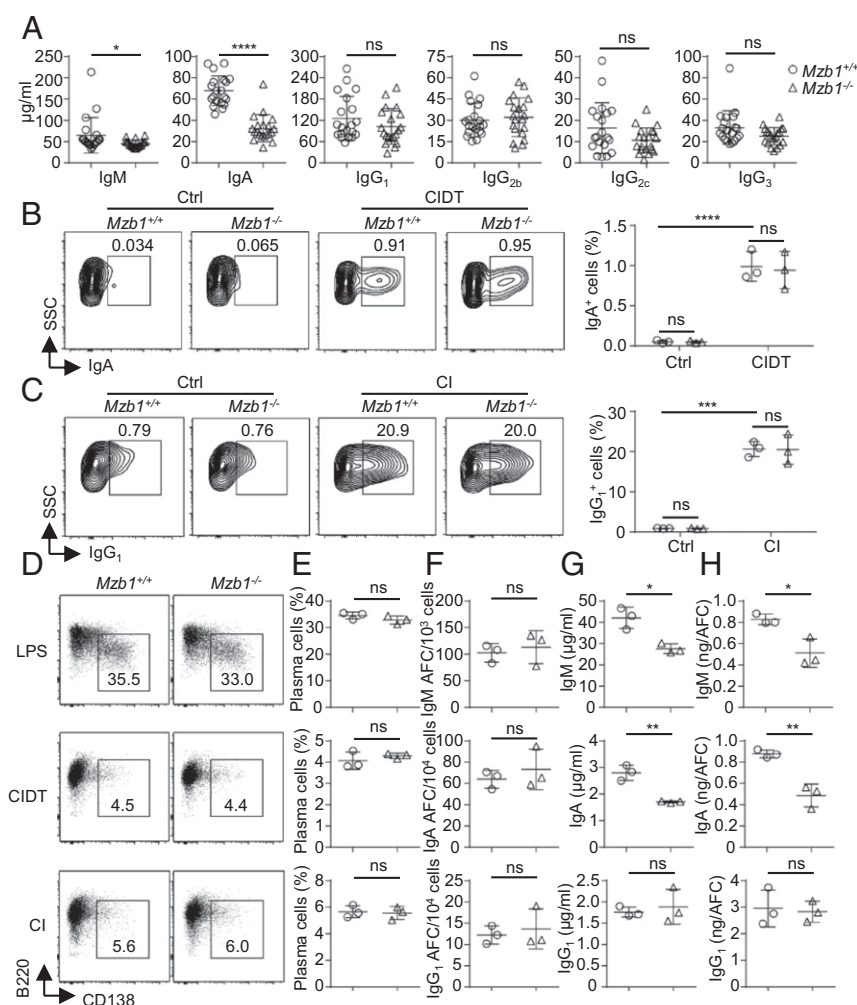
Fig. 1. MZB1 is required for efficient secretion of IgA and IgM, but not IgG, in vitro. (*A*) Reduced serum IgA and IgM levels in MZB1-deficient mice. Twenty pairs of age-matched $Mzb1^{+/+}$ and $Mzb1^{-/-}$ mice were bled, and serum Ig levels were measured by ELISA. (*B* and *C*) MZB1 deficiency does not affect CSR to IgA or IgG_1. Purified spleen B cells were cultured for 72 h with CD40 ligand–CD8a (1/2 volume), 2 μg/mL α-hCD8a, 10 ng/mL IL-4, 3 ng/mL dextran-conjugated α-IgD, and 2 ng/mL TGFβ (CIDT) to induce CSR to IgA, or CD40 ligand + IL-4 (CI) to induce CSR to IgG_1, and analyzed by flow cytometry. Fresh purified spleen B cells were used as a control (Ctrl). SSC, side scatter. (*B*) CSR to IgA. (*C*) CSR to IgG_1. Representative results of three independent experiments are shown. Means ± SD of three experiments are indicated in *B* and *C*, *Right*. (*D–H*) MZB1 promotes the secretion of IgA and IgM, but not IgG. Spleen B cells were purified and cultured for 4 d with LPS (*D–H*, *Top*; for production of IgM), CIDT (*D–H*, *Middle*; for production of IgA), and CI (*D–H*, *Bottom*; for production of IgG_1). (*D*) Representative profiles showing $B220^{low}CD138^+$ plasma cells. (*E*) Summary of three independent experiments shown in *D*. (*F*) ELISPOT assay for AFC (*Top*, IgM-AFC; *Middle*, IgA-AFC; *Bottom*, IgG_1-AFC). (*G*) The amount of Ab in the culture supernatants was analyzed by ELISA (*Top*, IgM; *Middle*, IgA; *Bottom*, IgG_1). (*H*) The average amount of Ab secreted by each AFC, calculated based on the results of *F* and *G*. Means ± SD of three experiments are shown. ns, not significant. *$P < 0.05$; **$P < 0.01$; ***$P < 0.001$; ****$P < 0.0001$ (two-tailed unpaired Student's *t* test).

differentiation of B cells into Ab-secreting plasma cells was not affected by the *Mzb1* mutation, we further performed enzyme-linked immunospot (ELISPOT) assays and confirmed that *Mzb1*^{+/+} and *Mzb1*^{−/−} B cells generated similar numbers of Ab-forming cells (AFCs) secreting IgM, IgA, or IgG$_1$ (Fig. 1F). In contrast, the concentration of IgM (Fig. 1 G, Top) and IgA (Fig. 1 G, Middle) in the culture supernatants of stimulated *Mzb1*^{−/−} B cells was significantly reduced compared with *Mzb1*^{+/+} B cells. Based on the number of plasma cells present in the culture (Fig. 1F) and the amount of Ab in the culture supernatant (Fig. 1G), it is clear that *Mzb1*^{−/−} plasma cells secreted less IgM and IgA on a per-cell basis, but normal amounts of IgG, compared with *Mzb1*^{+/+} plasma cells (Fig. 1H). These results demonstrate that MZB1 is involved in the secretion of IgA and IgM, but not IgG$_1$, by plasma cells under in vitro conditions.

To investigate whether MZB1 is also involved in the production of IgM and IgA in vivo, we first analyzed humoral immune responses against a T-independent (T-I) antigen (Ag) 4-hydroxy-3-nitrophenyl-acetyl–lipopolysaccharide (NP-LPS) and a T-dependent (T-D) Ag NP-chicken γ-globulin (NP-CGG). *Mzb1*^{−/−} mice produced significantly reduced levels of NP-specific IgM against both NP-LPS (Fig. 2A) and NP-CGG (Fig. 2B). In contrast, the production of NP-specific IgG$_1$ against NP-CGG was comparable between *Mzb1*^{+/+} and *Mzb1*^{−/−} mice during primary responses and after boosting (Fig. 2C). The proportion of germinal center B cells (B220^{+}CD38^{−}FAS^{+}) was similar in *Mzb1*^{+/+} and *Mzb1*^{−/−} mice at 12 d after NP-CGG immunization (Fig. 2D), suggesting that the reduced IgM production was not due to an impaired germinal center reaction.

Most IgA is secreted across mucous membranes, especially in the intestine (33). It has been shown that intraperitoneal (i.p.) injection of LPS induces increased secretion of IgA into the intestinal lumen (34, 35). Indeed, a robust increase of fecal IgA was observed at 24 h after i.p. administration of LPS to *Mzb1*^{+/+} mice (Fig. 2E). In striking contrast, LPS injection only induced a marginal increase of fecal IgA in *Mzb1*^{−/−} mice. These in vivo results demonstrate that MZB1 deficiency impaired the secretion of IgA into the gut in response to LPS stimulation.

MZB1 Binds to IgA via the αHC Secretory Tailpiece and Promotes Efficient Secretion of IgA.
To explore the molecular mechanism by which MZB1 is required for the secretion of IgA, we inactivated the *Mzb1* gene in the Ag8.653 plasmacytoma cell line (hereafter referred to as Ag8) by CRISPR/Cas9-mediated genome editing. Ag8 cells do not express endogenous Ig HC or LC but are capable of secreting high levels of Ab (36). By using two different guide RNAs that targeted exons 3 and 4, respectively (Fig. 3A), we established two MZB1-deficient clones, #5 and #9 (Fig. 3B and *SI Appendix*, Fig. S3). We then transduced these cells (#5 and #9) as well as control Ag8 cells with retrovirus expressing λ$_1$LC–internal ribosome entry site (IRES)–αHC or as a control λ$_1$LC–IRES–γ$_1$HC to allow the expression of IgA or IgG$_1$, respectively. We then compared the amount of IgA secreted from Ag8(α+λ$_1$), MZB1-deficient cells #5(α+λ$_1$) and #9(α+λ$_1$). As shown in Fig. 3C, the concentration of IgA in the supernatants of cells #5(α+λ$_1$) and #9(α+λ$_1$) was significantly lower than with Ag8(α+λ$_1$) cells cultured for 24–72 h. In contrast, Ag8(γ$_1$+λ$_1$), #5(γ$_1$+λ$_1$), and #9(γ$_1$+λ$_1$) cells secreted a very similar amount of IgG$_1$ in the supernatants after 24-, 48-, or 72-h culture (Fig. 3D). These results demonstrate that MZB1 deficiency specifically attenuated the secretion of IgA, but not IgG$_1$.

To further verify the role for MZB1 in IgA secretion by plasma cells, we reexpressed MZB1 in MZB1-deficient #9(α+λ$_1$) cells (*SI Appendix*, Fig. S3E). As shown in Fig. 3E, #9(α+λ$_1$) cells transduced with MZB1–IRES–green fluorescent protein (GFP), but not those transduced with GFP alone, expressed MZB1. In addition, MZB1^{high} cells expressed higher levels of MZB1 than MZB1^{low} cells. We then cultured these cells and measured the amount of IgA in the culture supernatants at different time points. As shown in Fig. 3F, reexpression of MZB1, but not GFP, in #9(α+λ$_1$) cells increased the amount of IgA in the supernatants.
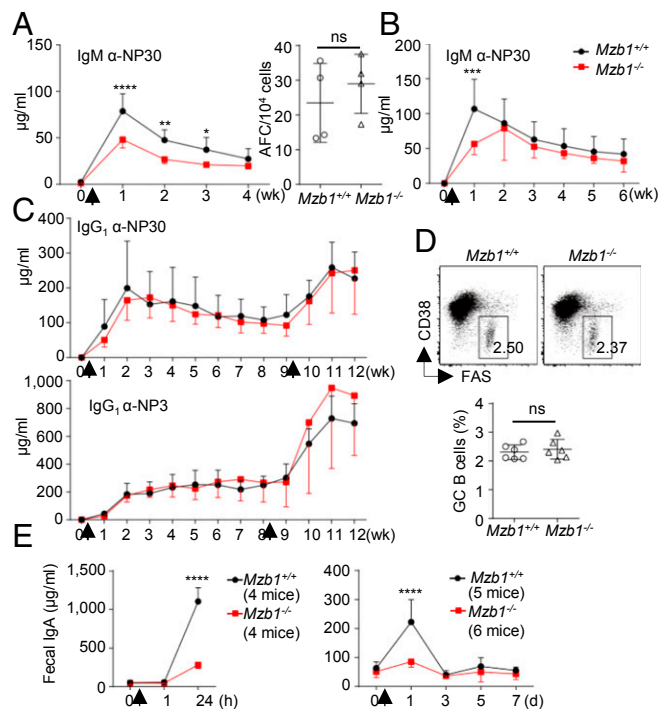
Fig. 2. MZB1 is required for efficient production of IgM and IgA, but not IgG$_1$, in vivo. (A, Left) Five pairs of *Mzb1*^{+/+} and *Mzb1*^{−/−} mice were immunized with 25 μg of NP-LPS and analyzed for the production of NP-specific IgM in the serum at 1–4 wk after immunization. (A, Right) ELISPOT assay for IgM AFC in the spleen at 1 wk postimmunization. (B and C) Eight pairs of *Mzb1*^{+/+} and *Mzb1*^{−/−} mice were immunized with 25 μg of NP-CGG in alum at week 0 and boosted with the same amount of NP-CGG in PBS 9 wk later. Serum levels of NP-specific IgM (B) and low-affinity (C, Upper) and high-affinity (C, Lower) NP-specific IgG$_1$ were measured at the indicated time points by ELISA. (D, Upper) FACS profiles showing GC B cells (B220^{+}CD38^{−}FAS^{+}) in the spleen at 12 d after immunization with 25 μg of NP-CGG in alum. (D, Lower) Mean ± SD of six pairs of *Mzb1*^{+/+} and *Mzb1*^{−/−} mice. (E) *Mzb1*^{−/−} mice are impaired in secreting IgA into the gut in response to acute inflammation. Four pairs of *Mzb1*^{+/+} and *Mzb1*^{−/−} (E, Left) and five *Mzb1*^{+/+} and six *Mzb1*^{−/−} mice (E, Right) were injected i.p. with 20 μg of LPS (arrowheads), and the fecal IgA was analyzed at the indicated time points by ELISA. Means ± SD are shown. ns, not significant. *P < 0.05; **P < 0.001; ***P < 0.001; ****P < 0.0001 (two-tailed unpaired Student's t test).

In addition, MZB1^{high} cells secreted higher levels of IgA than did MZB1^{low} cells. These results provide compelling evidence that MZB1 is required for efficient secretion of IgA in Ag8 plasmacytoma cells, but is not required for IgG$_1$ secretion.

To gain insights into the mechanism by which MZB1 promotes IgA secretion, we first examined whether MZB1 physically interacted with IgA. We immunoprecipitated IgA from Ag8(α+λ$_1$) and IgG$_1$ from Ag8(γ$_1$+λ$_1$) cells and found that BiP was coprecipitated with both IgA (Fig. 3G) and IgG$_1$ (Fig. 3H), consistent with earlier findings that BiP binds to the HC of both IgA and IgG (37, 38). In contrast, MZB1 was coprecipitated with IgA (Fig. 3G), but not IgG$_1$ (Fig. 3H). The fact that Ag8(α+λ$_1$) and Ag8(γ$_1$+λ$_1$) expressed the same λ$_1$ LC suggested that MZB1 bound to the αHC, but not LC. GRP94, a cochaperone of BiP, was not associated with either IgA or IgG$_1$, consistent with the previous finding that it could be coimmunoprecipitated with Ig-HC only in the presence of a cross-linking agent (30, 39). These results demonstrate that MZB1 interacts with IgA through the αHC, but does not interact with IgG$_1$.

One of the main differences between IgA and IgG is that IgA, like IgM, possesses a secretory tailpiece in the secretory form of αHC (αtp) (22). The αtp, especially the penultimate residue Cys, is important for the oligomerization, folding, and degradation of IgA (40). We then asked whether the αtp could be involved in

Xiong et al.
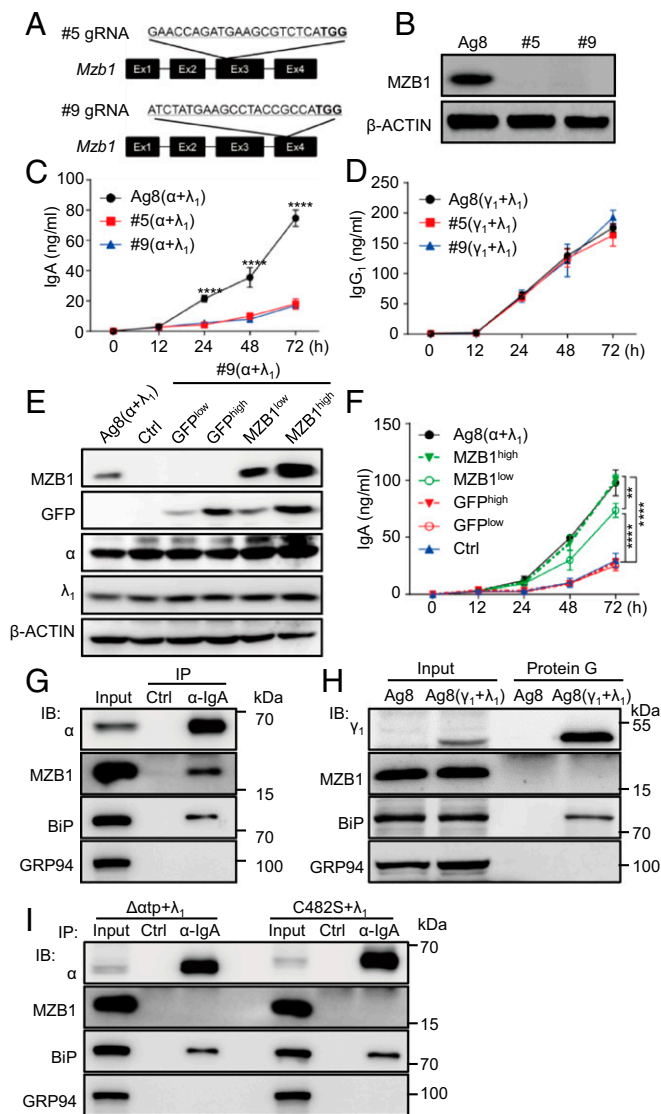
Fig. 3. MZB1 binds to IgA via the αtp dependent on the penultimate Cys (C482). (A and B) Generation of MZB1-deficient Ag8 cells. (A) Positions and sequences of two guide RNAs. (B) Immunoblot for MZB1 expression in MZB1-deficient Ag8 clones, #5 and #9, derived from #5 and #9 gRNA, respectively. (C and D) Ag8, #5, and #9 cells were transduced with retrovirus expressing α+λ$_1$ or γ$_1$+λ$_1$, and the levels of IgA (C) or IgG$_1$ (D) in the culture supernatants were measured at the indicated time points by ELISA. (E and F) Reexpression of MZB1 in MZB1-deficient #9(α+λ$_1$) cells restores normal IgA secretion. The #9(α+λ$_1$) cells were transduced with retrovirus expressing MZB1–IRES–GFP or GFP alone (SI Appendix, Fig. S3). Ag8(α+λ$_1$) cells were used as a control. (E) Immunoblot analysis for MZB1, GFP, αHC, λ$_1$LC, and β-actin protein expression. (F) The levels of IgA in the culture supernatants. (G–I) MZB1 interacts with IgA via αtp dependent on the penultimate Cys (C482). (G) MZB1 physically interacted with IgA. Ag8(α+λ$_1$) cells were lysed and immunoprecipitated with α-IgA Ab. Normal goat IgG was used as a negative control (Ctrl), and whole-cell lysate was used as input. Immunoblot was probed with α-IgA, -MZB1, -BiP, or -GRP94 Ab. (H) MZB1 did not interact with IgG$_1$. Ag8 and Ag8(γ$_1$+λ$_1$) cells were lysed, and IgG$_1$ was immunoprecipitated. Whole-cell lysate was used as input. Immunoblot was performed as in G. (I) MZB1 did not interact with IgA lacking the αtp (Δαtp) or IgA with mutated αtp (penultimate Cys mutated to Ser, C482S). Ag8 cells expressing Δαtp or C482S were lysed and immunoprecipitated with α-IgA Ab. Immunoblot was performed as in G. Means ± SD are shown. **P < 0.01; ****P < 0.0001 (two-tailed unpaired Student's t test for C and D; repeated-measures ANOVA for F).

MZB1 binding to IgA. We constructed two mutant αHCs, Δαtp, in which the 18-amino-acid secretory tailpiece was deleted, and C482S, in which the penultimate Cys residue in the tailpiece was mutated to Ser. We found that MZB1 failed to bind to either Δαtp or C482S, while BiP was still able to bind to these mutant αHCs (Fig. 3I). Therefore, MZB1 binds to IgA via its HC tailpiece.

MZB1 Stabilizes αHC–λ$_1$LC Complexes. We initially noted that MZB1 reexpression in #9(α+λ$_1$) cells increased αHC levels in proportion to the MZB1 expression levels (Fig. 3E, compare the amount of αHC in MZB1^{low} and MZB1^{high} lanes). To examine whether MZB1 is involved in maintaining the stability of αHC and λ$_1$LC, we treated Ag8(α+λ$_1$) and #5(α+λ$_1$) cells with cycloheximide (CHX) to block new protein synthesis and analyzed the amount of αHC and λ$_1$LC at different time points. We found that both αHC and λ$_1$LC were more rapidly degraded in the MZB1-deficient #5(α+λ$_1$) cells (Fig. 4A). Quantification of αHC and λ$_1$LC band intensities from three independent experiments revealed that >60% of the αHC was degraded by 12 h in the absence of MZB1, whereas no obvious degradation was observed in the presence of MZB1 (Fig. 4 A, Center). Similarly, λ$_1$LC was also more rapidly degraded in the absence of MZB1 (Fig. 4 A, Right). Since MZB1 interacted with αtp, but not with λ$_1$LC, the increased degradation of λ$_1$LC in the absence of MZB1 suggested that MZB1 stabilized the αHC–λ$_1$LC complexes. To verify this point, we expressed αHC alone in Ag8 or #5 cells and compared its half-life. We found that αHC, in the absence of the λ$_1$LC, was extremely stable, irrespective of MZB1 expression (Fig. 4B), possibly through interaction with BiP. These results demonstrate that MZB1 interacts with αtp and prevents the degradation of the αL complexes.

Although MZB1 was able to interact with αHC in the absence of LC (Fig. 4C), it interacted more strongly with αHC when LC was present (Fig. 3G). To more directly compare the relative binding of MZB1 and BiP to αHC, we immunoprecipitated αHC from Ag8 cells expressing α+λ$_1$ or α alone and analyzed the amount of coprecipitated MZB1 and BiP (Fig. 4 D, Left). Quantification of the amount of αHC, MZB1, and BiP revealed that 10 times more MZB1 bound to αHC when λ$_1$ was present than when λ$_1$ was absent (Fig. 4 D, Right). These observations suggest that MZB1 mainly interacts with HC–LC complexes in contrast to BiP, which mainly interacts with HC not associated with LC.

MZB1 Promotes the Secretion of Dimeric IgA. Having found that MZB1 interacts with IgA through αtp and promotes the stability of αL complexes, we next investigated whether MZB1 promoted the secretion of dimeric IgA. Comparison of the amount of IgA, Δαtp, and C482S secreted from Ag8 and #5 cells revealed that the absence of MZB1 (#5 cells) specifically attenuated the secretion of wild-type (WT) IgA (Fig. 5 A, Left), which was predominantly dimers (Fig. 5B), but not mutant IgA (Fig. 5 A, Center and Right), which were monomers (Fig. 5B). These results collectively suggest that the absence of MZB1 specifically attenuated the secretion of dimeric IgA.

To directly verify that MZB1 promoted the secretion of dimeric IgA, we collected culture supernatants of Ag8, Ag8(α+λ$_1$), and #5(α+λ$_1$) and measured the amount of IgA by enzyme-linked immunosorbent assay (ELISA). Supernatants containing equal amounts of IgA and control supernatant of Ag8 were then fractionated by nonreducing sodium dodecyl sulfate/polyacrylamide gel electrophoresis (SDS/PAGE). Immunoblot with horseradish peroxidase (HRP)-conjugated α-IgA detected dimeric (red arrowheads) and monomeric (blue arrowheads) IgA in the supernatants of Ag8(α+λ$_1$) and #5(α+λ$_1$) (Fig. 6 A, Left). Quantification of the relative band intensities of the dimeric and monomeric forms revealed that the proportion of dimeric IgA was reduced by 70% in #5(α+λ$_1$) compared with Ag8(α+λ$_1$) (Fig. 6 A, Right). Furthermore, when the same amount of serum IgA from three pairs of Mzb1$^{+/+}$ and Mzb1$^{-/-}$ mice was fractionated and blotted with α-IgA Ab, we
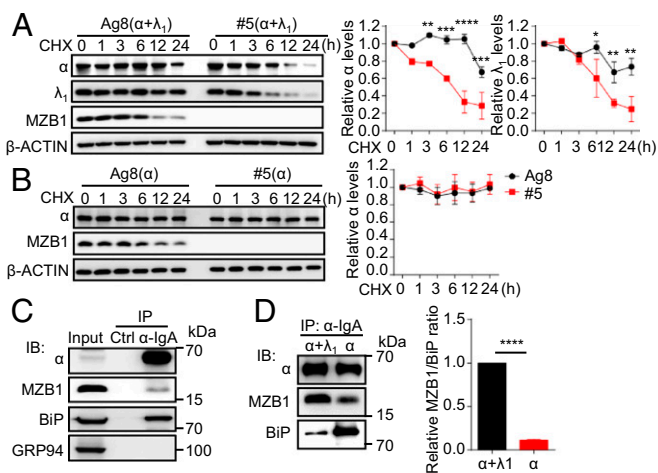
Fig. 4. MZB1 prevents the degradation of αL complexes. (*A*) Ag8(α+λ₁) and #5(α+λ₁) cells were treated with 10 μM CHX. The cells were then lysed at the indicated time points and blotted with α-αHC, α-λ₁LC, α-MZB1, or α-β-actin. (*A*, *Left*) Representative results. (*A*, *Center* and *Right*) Mean ± SD of three independent experiments. (*B*) MZB1 did not affect the stability of αHC when light chain was absent. Ag8 and #5 cells were transduced with αHC alone and analyzed for their stability, as in *A*. (*C* and *D*) MZB1 mainly bound to αL complexes, but not αHC alone, while BiP mainly bound to αHC alone, but not HC–LC complexes. (*C*) αHC was immunoprecipitated from Ag8(α) (αHC alone) with α-IgA and analyzed for the coprecipitation of MZB1, BiP, and GRP94. (*D*) αHC was immunoprecipitated from Ag8(α+λ₁) or Ag8(α) (αHC alone) with α-IgA and analyzed for the coprecipitation of MZB1 and BiP. The amount of MZB1 and BiP relative to the amount of precipitated αHC was quantitated. *$P < 0.05$; **$P < 0.01$; ***$P < 0.001$; ****$P < 0.0001$ (two-tailed unpaired Student's t test).

found that the dimeric IgA was also reduced by >50% in the sera from $Mzb1^{-/-}$ mice compared with those from WT mice, with the amount of monomeric IgA increased by more than twofold (Fig. 6*B*). These results demonstrate that MZB1 is required for efficient secretion of the dimeric, but not monomeric, IgA.

MZB1 Promotes J-Chain Incorporation into IgA. We have shown that MZB1 interacts with IgA through the αtp. Notably, the αtp is known to bind the J chain, a 15-kDa protein component required for the secretion of IgA into the mucosa. We therefore investigated whether MZB1 plays a role in J-chain incorporation into IgA. Culture supernatants used in Fig. 6*A* were resolved by nonreducing SDS/PAGE and blotted with α-J-chain Ab. As shown in Fig. 6*C*, the J chain was predominantly detected in dimeric IgA (red arrowheads), with only a faint band detectable in monomeric IgA (blue arrowheads). Quantification of the J-chain band intensities from three experiments revealed a significant reduction in the amount of J chain bound to IgA secreted by MZB1-deficient #5 cells (Fig. 6 *C*, *Right*). In addition, the sera used in Fig. 6*B* were also resolved by nonreducing SDS/PAGE and blotted with α-J-chain Ab, and, again, the amount of J chain in dimeric IgA was significantly reduced in sera from $Mzb1^{-/-}$ mice compared with those from $Mzb1^{+/+}$ mice (Fig. 6*D*).

To explore how MZB1 affected J-chain binding to IgA, we further analyzed intracellular J-chain–IgA association. Cell lysates of Ag8, Ag8 expressing αHC alone, #5(α+λ₁), and Ag8(α+λ₁) were resolved by nonreducing SDS/PAGE and blotted with α-IgA and α-J-chain Ab. As shown in Fig. 6*E*, a strong monomeric (blue arrowheads), but only a faint dimeric (red arrowheads), IgA band was detected by α-IgA Ab (Fig. 6 *E*, *Left*). The relatively low amount of dimeric IgA compared with monomeric IgA is consistent with earlier observations (41–43), which suggested that dimeric IgA is secreted as soon as it forms a dimer. Immunoblot with α-J-chain Ab detected a strong and a weak J-chain band in the

dimeric and monomeric IgA, respectively, in the lysate of Ag8(α+λ₁) (Fig. 6 *E*, *Right*). In contrast, a J-chain band was barely detectable in the lysate of #5(α+λ₁) cells (Fig. 6*E*, *Right*). These results demonstrate that MZB1 promotes J-chain binding to IgA before IgA secretion. In contrast to the severely reduced J-chain association with the intracellular IgA in #5(α+λ₁) cells (Fig. 6 *E*, *Right*), a J-chain band was detectable in the dimeric IgA secreted from #5(α+λ₁) cells (Fig. 6*C*). We think that #5(α+λ₁) cells may favor the secretion of J-chain–containing IgA. To explore whether MZB1 might interact with the J chain directly or indirectly, we immunoprecipitated the J chain and found that MZB1 could not be coprecipitated (Fig. 6*F*). These observations suggest that MZB1 and the J chain do not bind to IgA simultaneously.

MZB1-Deficient Mice Show Increased Susceptibility to DSS-Induced Colitis. pIgR mediates epithelial transport of J-chain–containing dimeric IgA to mucosal surfaces, which is important for mucosal immunity (44). Consistent with the impaired IgA secretion into the gut (Fig. 2*E*), $Mzb1^{-/-}$ mice were significantly more sensitive to DSS-induced colitis than $Mzb1^{+/+}$ mice, as revealed by greater body-weight loss (Fig. 7*A*), higher disease activity index score (Fig. 7*B*), and shorter colon length (Fig. 7*C*). Histological examination revealed increased inflammatory cell infiltration and extensive loss of tissue integrity in the colon of $Mzb1^{-/-}$ mice compared with $Mzb1^{+/+}$ mice (Fig. 7*D*). In addition, two $Mzb1^{-/-}$ mice died by day 10, whereas all of the $Mzb1^{+/+}$ mice survived during the course of DSS-induced colitis, consistent with the increased susceptibility to DSS-induced colitis in $Mzb1^{-/-}$ mice. We performed these experiments three times, and the data of the two other experiments are shown in *SI Appendix*, Fig. S4.

To explore whether the severe colitis observed in $Mzb1^{-/-}$ mice was associated with reduced IgA levels in the gut, we measured IgA and IgM levels in feces of $Mzb1^{+/+}$ and $Mzb1^{-/-}$ mice (Fig. 7 *E* and *F*). After DSS administration, the levels of both IgA (Fig. 7*E*) and IgM (Fig. 7*F*) were increased at days 4 and 10 in the gut of $Mzb1^{+/+}$ mice. In striking contrast, the levels of IgA were not increased (Fig. 7*E*), and IgM increased only marginally in $Mzb1^{-/-}$ mice (Fig. 7*F*). It should be noted that the levels of fecal IgA and IgM were similar in $Mzb1^{+/+}$ and $Mzb1^{-/-}$ mice at the steady state before DSS administration (Fig. 7 *E* and *F*, day 0). Therefore,
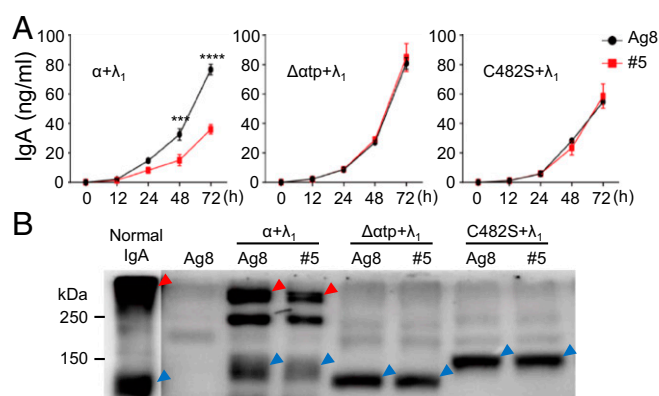
Fig. 5. MZB1 promotes the secretion of WT, but not mutant IgA (Δαtp and C482S). (*A*) Ag8 or MZB1-deficient #5 cells were transduced with retrovirus expressing α+λ₁, Δαtp+λ₁, or C482S+λ₁ and analyzed for the levels of IgA in the culture supernatants at the indicated time points. Means ± SD of three experiments are shown. (*B*) Immunoblot analysis of IgA in the culture supernatants of Ag8 and #5 cells expressing α+λ₁, Δαtp+λ₁, or C482S+λ₁. Cells were cultured for 72 h, and the supernatants were collected, fractionated by nonreducing SDS/PAGE, and blotted with α-IgA. Normal IgA (catalog No. S107; SouthernBiotech) was used as a control. Dimeric and monomeric IgA are indicated by red and blue arrowheads, respectively. ***$P < 0.001$; ****$P < 0.0001$ (two-tailed unpaired Student's t test).
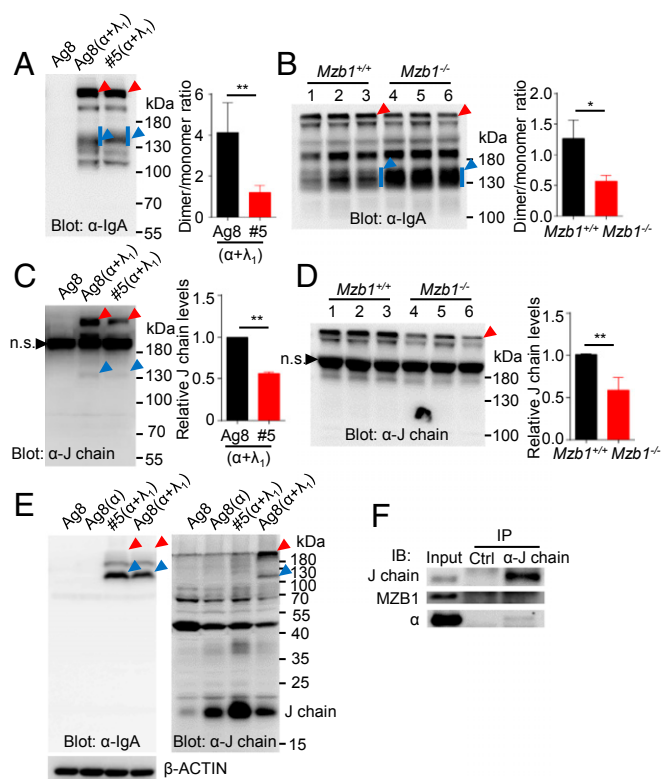
Fig. 6. MZB1 promotes the secretion of J-chain–containing dimeric IgA. (*A* and *B*) MZB1 promotes the secretion of dimeric IgA. (*A*) Culture supernatants of Ag8($\alpha+\lambda_1$) and #5($\alpha+\lambda_1$) (containing equal amounts of IgA) were analyzed for the amount of dimeric and monomeric IgA by nonreducing SDS/PAGE. (*A*, *Left*) Immunoblot. (*A*, *Right*) Mean ± SD of two independent experiments. (*B*) Sera from three pairs of *Mzb1*$^{+/+}$ and *Mzb1*$^{-/-}$ mice (containing equal amounts of IgA) were analyzed for the dimeric and monomeric IgA. (*B*, *Left*) Immunoblot. (*B*, *Right*) Mean ± SD of three mice. (*C–E*) MZB1 promotes J-chain association with IgA. (*C*) Culture supernatants used in *A* were blotted with α-J chain. (*C*, *Left*) Representative results. (*C*, *Right*) Mean ± SD of two independent experiments. (*D*) Sera used in *B* were blotted with α-J chain. (*D*, *Left*) Immunoblot. (*D*, *Right*) Mean ± SD. (*E*) Absence of MZB1 resulted in severely reduced J-chain association with the intracellular IgA. Ag8, Ag8 expressing αHC alone, #5 expressing $\alpha+\lambda_1$, and Ag8 expressing $\alpha+\lambda_1$ were lysed, fractionated by nonreducing SDS/PAGE, and blotted with α-IgA (*E*, *Left*) or α-J chain (*E*, *Right*). (*F*) MZB1 and the J chain do not interact with each other directly or indirectly. The J chain was precipitated from J558 cells (which express IgA) and blotted with α-MZB1 and -IgA. Red and blue arrowheads indicate dimeric and monomeric IgA, respectively. n.s., nonspecific. *$P < 0.05$; **$P < 0.01$ (two-tailed unpaired Student's *t* test).

MZB1 is particularly required for the rapid secretion of IgA and IgM into the gut under inflammatory conditions.

IgA Administration Restores the Normal Sensitivity to DSS-Induced Colitis in *Mzb1*$^{-/-}$ Mice. IgA is the major Ab isotype in luminal secretions, especially the gut lumen, and is crucial in protecting the integrity of the intestinal barrier (2, 3, 45). To further confirm that the severe colitis observed in *Mzb1*$^{-/-}$ mice was due to reduced IgA production in the gut, mice were fed with a monoclonal IgA Ab, W27, before and after DSS administration. W27 is a high-affinity polyreactive IgA derived from plasma cells in the mouse intestinal lamina propria and is a gut commensal modulator (15). W27 bound to multiple bacteria and could suppress the growth of *Escherichia coli*, but did not bind to and suppress the growth of beneficial bacteria, such as *Lactobacillus casei*. Intriguingly, W27 oral administration significantly ameliorated DSS-induced colitis in *Mzb1*$^{-/-}$ mice (Fig. 7 *G–J*), with less body-weight loss (Fig. 7*G*), reduced disease activity index score (Fig. 7*H*), and longer colon length (Fig. 7*I*) compared

with the control group. Histological analysis revealed less inflammatory cell infiltration, and the mucosal tissue was almost intact in the W27-treated group (Fig. 7*J*). In contrast, oral administration of W27 had no effect on the severity of DSS-induced colitis in *Mzb1*$^{+/+}$ mice (Fig. 7 *K–N*), indicating that the amount of IgA in the gut of *Mzb1*$^{+/+}$ mice is already sufficient and that administration of exogenous IgA did not further protect the mice against DSS-induced inflammation and colitis. These results demonstrate that MZB1-mediated efficient IgA secretion is crucial for the suppression of gut inflammation.
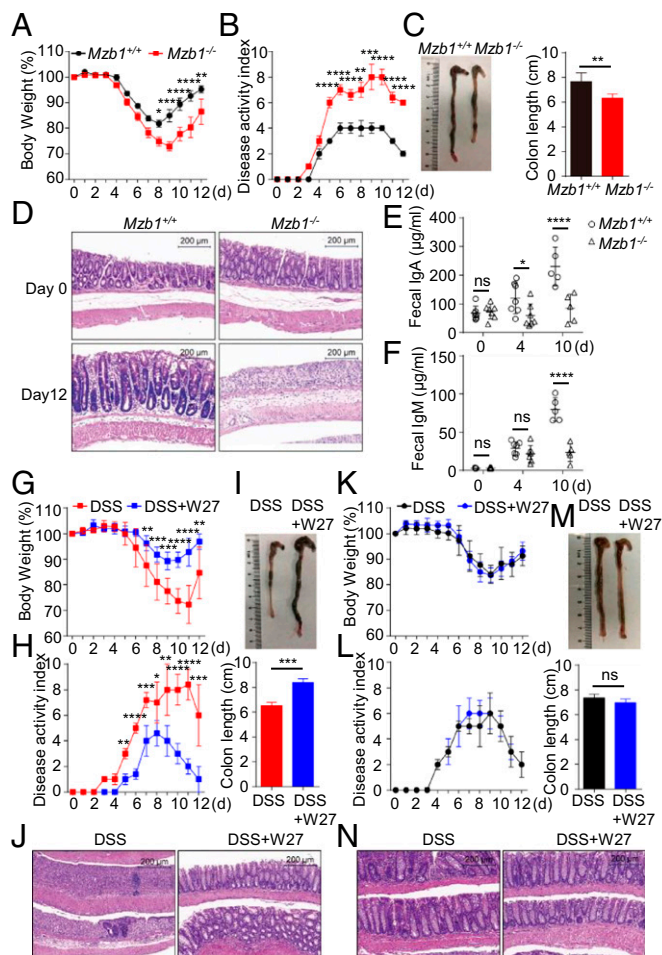
Fig. 7. MZB1-deficient mice are highly sensitive to DSS-induced colitis due to the inability to secrete IgA into the gut. (*A–D*) MZB1-deficient mice are highly sensitive to DSS-induced colitis. Acute colitis was induced in *Mzb1*$^{+/+}$ and *Mzb1*$^{-/-}$ mice by administration of 2.5% DSS in the drinking water for 6 d followed by regular drinking water for an additional 6 d. (*A*) Body weight of mice was monitored daily. (*B*) Disease activity index scores. (*C*) Colon length at the end of the experiments (day 12). (*D*) Representative hematoxylin and eosin staining of colon sections before and after DSS administration. (*E* and *F*) MZB1-deficient mice are unable to up-regulate fecal IgA and IgM during DSS-induced colitis. The levels of IgA (*E*) and IgM (*F*) in feces at days 0, 4, and 10 after DSS treatment were measured by ELISA. Means ± SD of the results from 5–7 *Mzb1*$^{+/+}$ and *Mzb1*$^{-/-}$ mice are shown. (*G–N*) Administration of a monoclonal IgA, W27, ameliorates the colitis in MZB1-deficient mice. *Mzb1*$^{-/-}$ (*G–J*) and *Mzb1*$^{+/+}$ (*K–N*) mice were fed with DSS alone or DSS+W27. W27 was administered in drinking water at a concentration of 25 μg/mL for 3 d and then together with 2.5% DSS for 6 d, followed by normal drinking water for an additional 6 d. Colitis severity was shown by body weight loss (*G* and *K*), disease activity index scores (*H* and *L*), decrease in colon length (*I* and *M*), and colon histopathology change (*J* and *N*). Means ± SD of 8–10 mice are shown. ns, not significant. *$P < 0.05$; **$P < 0.01$; ***$P < 0.001$; ****$P < 0.0001$ (two-tailed unpaired Student's *t* test).

MZB1 Affects the Microbiota Composition in the Gut During DSS-Induced Colitis. IgA plays an important role in maintaining a healthy composition of the gut microbiota. We next analyzed whether MZB1 deficiency affected gut microbiota before and after DSS-induced colitis. We found a similar composition of the fecal microbiota in $Mzb1^{+/+}$ and $Mzb1^{-/-}$ mice before DSS administration (*SI Appendix,* Fig. S5), consistent with the finding that the fecal IgA levels in $Mzb1^{+/+}$ and $Mzb1^{-/-}$ mice were comparable at the steady state (Fig. 7E). Four days after DSS administration, we found distinctive fecal microbiota in $Mzb1^{+/+}$ and $Mzb1^{-/-}$ mice (Fig. 8A). The relative abundance of three different bacterial phyla were significantly changed, with *Proteobacteria* and *Verrucomicrobia* being increased and *Bacteroidetes* being reduced in $Mzb1^{-/-}$ mice compared with $Mzb1^{+/+}$ mice (Fig. 8B). At the genus level, we found a significant difference in the mean proportion of 12 different bacterial genera. Among them, we found a dramatic increase of *Akkermansia* and reduction of *Alloprevotella* in $Mzb1^{-/-}$ mice (Fig. 8C). It has been extensively reported that DSS-induced colitis is accompanied by dysbiosis (46, 47), and our data clearly show that MZB1 deficiency aggravated the dysbiosis in the course of DSS-induced colitis.

Administration of Monoclonal IgA Repressed the Expansion of *Akkermansia*. W27 administration reduced the sensitivity to DSS-induced colitis in $Mzb1^{-/-}$ mice. Therefore, we compared the microbiota composition in the gut of $Mzb1^{-/-}$ mice treated with DSS alone or DSS + W27. Four days after administration of DSS alone or DSS + W27, we found distinctive fecal microbiota between these groups (Fig. 8D). The relative abundance of *Verrucomicrobia* was significantly repressed in the DSS + W27 group compared with the DSS-only group (Fig. 8E). At the genus level, we found a significant difference in the mean proportion of 16 different bacterial genera (Fig. 8F). *Akkermansia* was significantly repressed by W27 and *Lactobacillus* (generally considered to be probiotic) was significantly expanded in the W27 + DSS group (Fig. 8F).

Discussion

IgA is the most abundant Ab produced in the body and plays a critical role in gut homeostasis and mucosal immunity. A number of molecules have been described that participate in the assembly or secretion of IgM and IgG, including BiP, PDI, GRP94, SIL1, and GRP170 (48, 49). It has been unclear, however, whether the production of large amounts of IgA requires specific or additional molecules. In the present study, we have identified MZB1 as a molecular chaperone that functions to stabilize intracellular αL complexes and promote J-chain binding to IgA and the secretion of dimeric IgA.

We found that MZB1 physically interacted with αHC via the αtp and was dependent on the penultimate Cys residue (C482). In contrast, BiP, a molecular chaperone required to retain free Ig HC in the ER and prevent its degradation, was able to bind to both Δαtp and C482S mutant IgA, in agreement with the earlier finding that BiP binds to the Ig CH1 domain. We also found that BiP bound much more strongly to αHC when LC was absent than when LC was present, which is also consistent with the notion that LC triggers BiP release from HC (50). In striking contrast, we found that MZB1 bound to αHC much more strongly when LC was present than when LC was absent. These observations suggest that BiP and MZB1 bind to αHC sequentially, dependent on the availability of LC, and that MZB1 function occurs after the HC–LC complex is formed. Consistent with this idea, we found that MZB1 did not affect the half-life of αHC when LC was not expressed, but only when both αHC and λ_1LC were expressed, MZB1 promoted their stability. Exactly how MZB1 enhances the stability of αL complexes remains to be investigated. One possibility is that MZB1 promotes the assembly of αHC and LC, thereby preventing the accumulation and degradation of incorrectly folded αL complexes.

Fig. 8. Oral administration of W27 to $Mzb1^{-/-}$ mice during DSS-induced colitis normalizes their microbiota composition. (*A–C*) Differential composition of microbiota in $Mzb1^{+/+}$ and $Mzb1^{-/-}$ mice at day 4 after DSS treatment. DSS was administered as in Fig. 7 *A–D*, and 4 d later, stool samples from $Mzb1^{+/+}$ and $Mzb1^{-/-}$ mice were subjected to 16S V4 rDNA gene sequencing (four mice per group). (*A*) Principal coordinate analysis (PCA) illustrating degree of variance for the indicated mice within each group. (*B*) Relative abundance of bacterial phyla present in feces. (*C*) Differential abundance testing is used to identify bacterial genera that differ between the indicated groups. (*D–F*) Oral administration of W27 to $Mzb1^{-/-}$ mice during DSS-induced colitis normalizes their microbiota composition. DSS and W27 were administered to $Mzb1^{-/-}$ mice as in Fig. 7 *G–J*. Stool samples were collected from $Mzb1^{-/-}$ mice treated with DSS alone or DSS+W27 for 4 d and subjected to 16S V4 rDNA gene sequencing (four mice per group). (*D*) PCA illustrating degree of variance for the indicated mice within each group. (*E*) Relative abundance of bacterial phyla present in feces. (*F*) Differential abundance testing is used to identify bacterial genera that differ between the indicated groups. # indicates the major bacterial phyla found in the feces. Bacterial genera that differ significantly among two groups are shown in red ($P < 0.05$, Welch's t test).

The αtp, especially the penultimate Cys residue (C482), has been shown to mediate J-chain binding and dimerization of IgA (40, 51), with each C482 on two IgA monomers forming a disulfide bond to Cys14 and Cys68 on the J chain, respectively. We found that αtp and C482 are also required for MZB1 binding to IgA. Therefore, MZB1 and the J chain bind to the same αtp. The difference is that MZB1 binds to the αtp noncovalently, whereas the J chain forms disulfide bonds with C482 of the αtp. However, MZB1 and the J chain did not coprecipitate (Fig. 6F), indicating that they do not bind to IgA simultaneously, but rather sequentially. MZB1 and the J chain are localized in the ER and cytoplasm, respectively, which suggests that MZB1 interacts with IgA before J-chain association. Based on these observations, we propose that by noncovalently binding to the tailpiece, MZB1 may maintain or create a structure that allows

efficient forming of the disulfide bonds between the penultimate Cys482 of the αtp and Cys14 or Cys68 on the J chain. Mutation of Cys482 to Ser might alter the structure of the tailpiece and thus disrupt the binding of MZB1. By extension, disulfide bond formation between Cys482 of the αtp and Cys14 or Cys68 on the J chain may displace MZB1 from the αtp. Further studies are required to clarify the molecular interactions among MZB1, the J chain, and IgA.

The J chain is considered to be involved in IgA dimer formation. Although mice lacking the J chain were able to produce dimeric IgA, these mice had at least 10 times more monomer than dimer in the serum, in contrast to the ~1:1 ratio of dimer/monomer observed in serum of WT mice (52). It has been suggested that the J chain promotes the efficiency of IgA dimer formation or plays a role in maintaining IgA dimer stability (52). We found that the absence of MZB1 reduced the dimeric and increased the monomeric IgA secretion in both Ag8 cells and in mice. One possibility is that by promoting J-chain binding to IgA, MZB1 indirectly contributes to IgA dimer formation. Alternatively, MZB1 may enhance IgA dimer formation independent of the J chain.

We found that IgA secretion in MZB1-deficient Ag8 cells was reduced by approximately three-quarters compared with WT Ag8 cells (Fig. 3C). Similarly, serum IgA levels were reduced by 52% in $Mzb1^{-/-}$ mice compared with $Mzb1^{+/+}$ mice (Fig. 1A). In addition to the overall reduction of IgA secretion in the absence of MZB1, the amount of the J chain contained in the secreted IgA was also reduced in both Ag8 cells and $Mzb1^{-/-}$ mice (Fig. 6). IgA can be produced in the gut lymphoid tissues and exported to the gut lumen. In addition, serum IgA can be transported to the intestine by the pIgR expressed on hepatocytes (53, 54). In both cases, the J chain is essential for pIgR-mediated IgA transcytosis. The dramatic decrease in LPS-induced fecal IgA (Fig. 2E) and failure to up-regulate IgA in the gut after DSS administration (Fig. 7E) in $Mzb1^{-/-}$ mice could be due to a combination of both decreased IgA secretion by plasma cells and reduced amount of J-chain association.

Based on our results and previous studies, we propose the following scheme for MZB1-mediated efficient IgA secretion (Fig. 9). The αHC is bound by BiP and retained in the ER, which prevents αHC degradation. BiP is then replaced by an Ig LC, and the resulting αL complexes are then bound and stabilized by MZB1 (as shown in Fig. 4A). MZB1 binding also promotes J-chain association with IgA and dimer formation (Fig. 6) by a yet-unknown mechanism. We think that BiP, MZB1, and the J chain bind sequentially to αHC to allow efficient secretion of J-chain–containing dimeric IgA.

MZB1 deficiency also impaired IgM production during both T-I and T-D humoral immune responses, which is consistent with the prior work showing that MZB1 is involved in the assembly of IgM (28) and contributes to the secretion of IgM in vitro (29) and in vivo (31, 55). In contrast to previous findings that MZB1 regulated cell proliferation (31), we found that MZB1-deficient primary B cells proliferated normally to various stimuli under in vitro conditions and that MZB1-deficient mice formed normal-sized GCs after immunization with a T-D Ag. Further studies are required to resolve these discrepancies. We also found that MZB1 deficiency did not affect Ig gene CSR or differentiation into plasma cells under both in vitro and in vivo conditions. Our results reveal a specific and critical role for MZB1 in the secretion of IgA and IgM, but not IgG, by plasma cells.

Although serum IgA levels were reduced in MZB1-deficient mice, IgA levels in the gut were comparable between $Mzb1^{+/+}$ and $Mzb1^{-/-}$ mice maintained under specific pathogen-free conditions. Previous studies have revealed that pIgR expression on gut epithelial cells is low at the steady state but strongly up-regulated by Toll-like receptor (TLR; including TLR4) signaling (56). It is thus possible that under normal noninflammatory
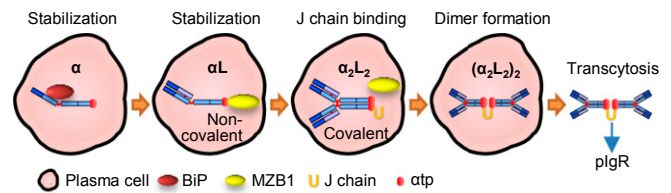
Fig. 9. A scheme illustrating the roles for BiP, MZB1, and the J chain in IgA biosynthesis and secretion. The free αHC is bound by BiP and retained in the ER, which prevents αHC degradation. An Ig LC triggers BiP release from HC, and the resulting αL complexes are then bound and stabilized by MZB1. MZB1 binding further promotes J-chain association with IgA and dimer formation by a yet-unknown mechanism. BiP, MZB1, and the J chain bind sequentially to αHC to allow efficient secretion of J-chain–containing dimeric IgA.

conditions, the amount of J-chain–containing IgA produced in the absence of MZB1 is sufficient and that the low level of pIgR expression is the limiting factor for IgA transport to the gut lumen. Under inflammatory conditions, pIgR expression is up-regulated, and more IgA-secreting plasma cells are generated. In this case, the decreased IgA secretion by plasma cells and reduced J-chain–IgA association caused by the absence of MZB1 would result in significantly impaired IgA transport to the gut. The inability to secrete large amounts of IgA in the gut exacerbated DSS-induced colitis. Our results are in agreement with earlier findings that fecal IgA increased following DSS treatment (57) and that there was a correlation between individual mice with lower levels of fecal IgA and severe colitis (58). Therefore, MZB1 is required for the maintenance of gut homeostasis, especially under inflammatory conditions.

IgA plays a critical role in modulating the intestinal microbiota, and IgA deficiency often leads to gut dysbiosis. We showed that MZB1 deficiency aggravated the dysbiosis in the course of DSS-induced colitis, with a dramatic increase of *Akkermansia* and reduction of *Alloprevotella*. *Akkermansia* is a mucin-degrading commensal and is known to exacerbate gut inflammation caused by *Salmonella* (59). Borton et al. (60) reported that *Akkermansia* was enriched in mouse feces following DSS treatment. *Alloprevotella* is a genus belonging to the family *Prevotellaceae*, which was reported to be a colitogenic bacteria (61) and exacerbated chemically induced colitis (62). However, *Alloprevotella* is a newly identified genus (63) and is a short-chain fatty acid (SCFA)-producing bacteria. SCFAs have been shown to play key functional roles in decreasing inflammation and enhancing mucosal barrier function (64). Therefore, the observed alterations in the composition of the intestinal microbiota are in line with the severe colitis observed in MZB1-deficient mice. Consistent with the possibility that the increased *Akkermansia* was related to the severe colitis, W27 administration to $Mzb1^{-/-}$ mice repressed *Akkermansia*, increased the *Lactobacillus*, and restored the normal sensitivity to DSS-induced colitis. In conclusion, the present study reveals an important mechanism that controls the quantity, quality, and function of IgA. Our findings provide a tool for efficient secretion of functional IgA and also have potential clinical applications.

Materials and Methods

Generation of $Mzb1^{-/-}$ Mice. A targeting vector was constructed to replace part of exon 1 and the remaining exons 2–4 of the *Mzb1* gene with a neomycin gene (*SI Appendix*, Fig. S1B). The targeting vector was linearized and transfected into C57BL/6-derived Bruce4 embryonic stem (ES) cells as described (65). The correctly targeted ES cells were identified by long-range genomic PCR and microinjected into C57BL/6 blastocysts. Blastocysts were transferred into pseudopregnant females, and resulting offspring were screened for germline transmission. Chimeric mice were generated and bred with C57BL/6 mice to obtain heterozygotes, which were further bred to obtain homozygotes. The mice were maintained under specific pathogen-free conditions in the animal facility of Fudan University. All animal experiments

and procedures were approved by the Animal Experiment Committee of Fudan University.

Flow Cytometry. Single-cell suspensions were obtained from the spleen, bone marrow, or peritoneal cavity of mice (8–12 wk old). The cells were first incubated with anti-CD16/32 (catalog No. 2.4G2; BD Biosciences) to block FcγR and then stained with following fluorochrome-conjugated Abs: α-B220 (catalog No. RA3-6B2; eBioscience), α-IgD (catalog No. 11-26c.2a; BioLegend), α-IgM (catalog No. AF6-78; BD Biosciences), α-CD21/35 (catalog No. 7G6; BD Biosciences), α-CD23 (catalog No. B3B4; BioLegend), α-CD5 (catalog No. 53-7.3; BD Biosciences), α-FAS (catalog No. Jo2; BD Biosciences), α-CD38 (catalog No. 90; BioLegend), α-IgG$_1$ (catalog No. RMG1-1; BioLegend), and α-IgA (catalog No. F9384; Sigma-Aldrich). For live vs. dead cell discrimination, we used 7-AAD Viability Staining Solution (eBioscience). For total IgA or IgG$_1$ staining, the cells were fixed with IC Fixation Buffer (eBioscience), permeabilized with Permeabilization Buffer (eBioscience), and stained with α-IgA or -IgG$_1$. Samples were analyzed with a FACSVerse flow cytometer (BD Biosciences) using the FACSuite software. Data analysis was performed by using FlowJo software (Treestar).

Cell Culture. Total spleen B cells were isolated by negative sorting with the IMag B cell purification kit (BD Biosciences) following manufacturer's instructions, and MZB (B220$^+$CD21^{hi}CD23$^-$) and follicular B (B220$^+$CD21^{int}CD23$^+$) cells were by sorted using a FACSAria (BD Biosciences). The Ag8.653 plasmacytoma cell line was obtained from ATCC. All cells were cultured in RPMI 1640 medium supplemented with 10% fetal bovine serum (FBS), 5×10^{-5} M 2-mercaptoethanol, 100 units/mL penicillin, and 100 μg/mL streptomycin (GIBCO).

Immunizations. For humoral immune responses, mice were immunized i.p. with 25 μg of NP-LPS (Biosearch Technologies) in 200 μL of phosphate-buffered saline (PBS) or 25 μg of NP-CGG (Biosearch Technologies) in 4.5% alum in 200 μL of PBS. For secondary responses to NP-CGG, mice were boosted with 25 μg of NP-CGG in PBS 9 wk later. NP-specific IgM and IgG$_1$ Abs were measured by ELISA as described (66). For inducing IgA production in the gut, mice were injected i.p. with 20 μg of LPS (*E. coli* O111:B4; Sigma-Aldrich) in 200 μL of PBS.

ELISA. ELISA was performed as described (59). Briefly, 96-well plates were coated with 50 μL per well of 2.5 μg/mL NP3- or NP30-bovine serum albumin (BSA) (Biosearch Technologies) for measuring high- and low-affinity NP-specific Abs, respectively. For measuring serum Ig, plates were coated with 5 μg/mL anti-Ig (H + L) (SouthernBiotech), and blocked with PBS containing 1% BSA for 1 h. Diluted samples were then added and incubated for 1 h at room temperature. After washing, HRP-conjugated goat α-mouse IgM, IgG$_1$, IgG$_{2b}$, IgG$_{2c}$, IgG$_3$, or IgA (SouthernBiotech) Abs were added and developed with 2,2′-azino-*bis*(3-ethylbenzothiazoline)-6-sulfonic acid solution. For detection of fecal Abs, fecal pellets were weighted and dissolved in PBS containing a protease inhibitor mixture (Sigma-Aldrich). Debris was removed by centrifugation. Fecal IgA was measured by a Mouse IgA ELISA Quantitation Set (Bethyl Laboratories).

ELISPOT Assay. Multiscreen high-throughput screening plates (Millipore) were coated with 50 μg/mL NP33-BSA or 5 μg/mL anti-Ig (H + L). Serially diluted cells were added to individual wells in triplicate and then incubated at 37 °C for 100 min in a CO$_2$ incubator. The plates were further incubated with alkaline phosphatase-conjugated goat anti-mouse IgM, IgA, or IgG$_1$ (SouthernBiotech). Spots were revealed by 5-bromo-4-chloro-3-indolyl phosphate/nitro blue tetrazolium reagent (MOSS Inc.), and colonies were counted by using an IMMUNOSPOT Analyzer (CTL Analyzers LLC).

Establishment of MZB1-Deficient Ag8 Cells. Two guide sequences, #5 (5′-GAACCAGATGAAGCGTCTCA-3′) and #9 (5′-ATCTATGAAGCCTACCGCCA-3′), targeting DNA within the third and fourth exons of the *Mzb1* gene, respectively, were designed by online software (http://www.crispr-cas.org/), which predicted high-specificity and protospacer adjacent motif target sites in the mouse exome. Construction of lentiCRISPR vector, generation of lentivirus, virus transduction into Ag8 cells, and selection of correctly targeted clones were performed essentially as described (67).

Construction of Expression Vectors for MZB1, IgA, and IgG$_1$. Amplification of various cDNA was performed with the high-fidelity KOD-plus polymerase (TOYOBO) to minimize PCR errors. Mouse *Mzb1* cDNA was amplified by using 5′-CGCGGATCCGCCACCATGAGACTGCCTCTGCCACTG-3′ and 5′-CCGGAATTCCTAAAGCTCTTCTCTCTGGGGC-3′ primers and first-strand cDNA generated from total RNA of Ag8 cells. After verifying the sequence, *Mzb1* cDNA was

subcloned into pMX-IRES-GFP retrovirus vector. Similarly, the open reading frames of Ig α HC, γ$_1$ HC and λ$_1$ LC were amplified by using first-strand cDNA generated from total RNA extracted from B1-8^{hi} (68) spleen B cells stimulated with CIDT or CI for 3 d in vitro. The following primers were used: B1-8^{hi} V$_H$ forward primer, 5′-CATGCCATGGGATGGAGCTGTATCATGC-3′; Cα reverse primer, 5′-ACGCGTCGACTCAGTAGCAGATGCCATCTCCC-3′; Cγ1 reverse primer, 5′-TCATTTACCAGGAGAGTGGGAGA-3′; Vλ1 forward primer, 5′-CGCGGATCCGCCACCATGGCCTGGATTTCACTTATACTCT-3′; Cλ1 reverse primer, 5′-CCGGAATTCCTAGGAACAGTCAGCACGGGAC-3′. The amplified products were subcloned into T vector and sequenced, and the correct clones were used. To express IgA and IgG$_1$, we deleted the GFP gene from the pMX-IRES-GFP retroviral vector and generated pMX-λ$_1$-IRES-α and pMX-λ$_1$-IRES-γ$_1$, respectively. Ag8 cells were transduced with retrovirus expressing IgA or IgG$_1$ as described (61). The transduced cells were subcloned by limiting dilution and analyzed for intracellular total IgA or IgG$_1$ expression.

Generation and Expression of IgA Lacking the Tailpiece (Δαtp) or with C482S Amino Acid Substitution. PrimeSTAR Mutagenesis Basal Kit (TaKaRa) was used to generate Δαtp and C482S. To generate Δαtp, primers 5′-GGTAAAT-GAACCAATGTCAGCGTGTCT-3′ and 5′-ATTGGTTCATTTACCCGACAGACG-GTC-3′ were used to change CCC (encoding the first amino acids of the tailpiece) to TGA (stop codon). To generate C482S, primers 5′-TGGCAT-CAGCTACTGAGTCGACGATA-3′ and 5′-CAGTAGCTGATGCCATCTCCCTCTGA-3′ were used to change TGC (the penultimate Cys) to AGC (Ser). These mutant αHC were used to construct pMX-λ$_1$-IRES-Δαtp and pMX-λ$_1$-IRES-C482S. Ag8 and MZB1-deficient #5 cells were transduced with retrovirus expressing GFP mixed with retrovirus expressing pMX-λ$_1$-IRES-Δαtp or pMX-λ$_1$-IRES-C482S at a ratio of 1:10, and the GFP$^+$ cells were sorted and used for further experiments.

Immunoblot and Immunoprecipitation. Cells were lysed with medium radio-immunoprecipitation assay lysis buffer (Cwbiotech) containing a protease inhibitor mixture. Lysates were mixed with sample buffer, boiled at 95 °C for 5 min, and separated by SDS/PAGE. Immunoblot was performed with specific Ab and secondary α-mouse or rabbit Ab conjugated to HRP. The membrane was developed with chemiluminescence. For detection of IgA under non-reducing conditions, samples were diluted in sample buffer without reducing agent, boiled at 95 °C for 1 min, separated by 7.5% SDS/PAGE, and detected by immunoblot.

For immunoprecipitation, cells were lysed with Nonidet P-40 lysis buffer (Beyotime) containing a protease inhibitor mixture. Precleared lysates were incubated with goat α-mouse IgA (SouthernBiotech) or goat normal IgG (Santa Cruz Biotechnology) overnight at 4 °C with mild rotation, and then Dynabeads Protein G (Invitrogen) were added and rotated for 4 h at 4 °C. After extensive washing with Nonidet P-40 lysis buffer, the precipitates were boiled in sample buffer and subjected to SDS/PAGE and immunoblot. The following Abs were used for immunoblot: HRP-α-mouse-IgA (SouthernBiotech), HRP-α-mouse-lambda (SouthernBiotech), α-GFP (catalog No. 1E4; Enzo Life Sciences), α-β-actin (catalog No. A1978; Sigma-Aldrich), α-BiP (catalog No. ab21685; Abcam), and α-GRP94 (catalog No. D6X2Q; CST). Polyclonal rabbit Ab against MZB1 were obtained by immunizing rabbits with a mixture of two peptides, LAKAEAKSHTPDASG and SAPTLDDEEKYS, corresponding to amino acids 63–77 and 29–40 of mouse MZB1, respectively.

DSS-Induced Colitis, W27 Oral Administration, and Determination of Gut Microbiota Composition. Colitis was induced by oral administration of 2.5% DSS (MP Biomedicals) for 6 d in the drinking water followed by normal drinking water. Disease activity index scores were determined as described (69). W27 is a monoclonal IgA described recently (15). W27 was administered in drinking water for 3 d and then together with 2.5% DSS for 6 d, followed by normal drinking water. Fecal samples were collected from colons of mice and sent to Sangon Biotech for sequencing the V4 region of the 16S rDNA gene. The results were analyzed as described (46).

Statistical Analysis. Statistical significance was assessed by two-tailed unpaired Student's *t* test, Welch's *t* test, or repeated-measures ANOVA (*$P < 0.05$; **$P < 0.01$; ***$P < 0.001$; ****$P < 0.0001$).

1. S. Fagarasan, T. Honjo, Intestinal IgA synthesis: Regulation of front-line body defences. *Nat. Rev. Immunol.* **3**, 63–72 (2003).
2. O. Pabst, New concepts in the generation and functions of IgA. *Nat. Rev. Immunol.* **12**, 821–832 (2012).
3. C. Gutzeit, G. Magri, A. Cerutti, Intestinal IgA production and its role in host-microbe interaction. *Immunol. Rev.* **260**, 76–85 (2014).
4. A. J. Macpherson, B. Yilmaz, J. P. Limenitakis, S. C. Ganal-Vonarburg, IgA function in relation to the intestinal microbiota. *Annu. Rev. Immunol.* **36**, 359–381 (2018).
5. L. Yel, Selective IgA deficiency. *J. Clin. Immunol.* **30**, 10–16 (2010).
6. A. Cerutti, K. Chen, A. Chorny, Immunoglobulin responses at the mucosal interface. *Annu. Rev. Immunol.* **29**, 273–293 (2011).
7. N. Wang, L. Hammarström, IgA deficiency: What is new? *Curr. Opin. Allergy Clin. Immunol.* **12**, 602–608 (2012).
8. J. Fadlallah *et al.*, Microbial ecology perturbation in human IgA deficiency. *Sci. Transl. Med.* **10**, eaan1217 (2018).
9. G. H. Jorgensen *et al.*, Clinical symptoms in adults with selective IgA deficiency: A case-control study. *J. Clin. Immunol.* **33**, 742–747 (2013).
10. S. Koskinen, Long-term follow-up of health in blood donors with primary selective IgA deficiency. *J. Clin. Immunol.* **16**, 165–170 (1996).
11. N. Lycke, L. Erlandsson, L. Ekman, K. Schön, T. Leanderson, Lack of J chain inhibits the transport of gut IgA and abrogates the development of intestinal antitoxic protection. *J. Immunol.* **163**, 913–919 (1999).
12. A. K. Murthy, C. N. Dubose, J. A. Banas, J. J. Coalson, B. P. Arulanandam, Contribution of polymeric immunoglobulin receptor to regulation of intestinal inflammation in dextran sulfate sodium-induced colitis. *J. Gastroenterol. Hepatol.* **21**, 1372–1380 (2006).
13. K. Suzuki *et al.*, Aberrant expansion of segmented filamentous bacteria in IgA-deficient gut. *Proc. Natl. Acad. Sci. U.S.A.* **101**, 1981–1986 (2004).
14. A. Nakajima *et al.*, IgA regulates the composition and metabolic function of gut microbiota by promoting symbiosis between bacteria. *J. Exp. Med.* **215**, 2019–2034 (2018).
15. S. Okai *et al.*, High-affinity monoclonal IgA regulates gut microbiota and prevents colitis in mice. *Nat. Microbiol.* **1**, 16103 (2016).
16. M. W. Russell, J. Reinholdt, M. Kilian, Anti-inflammatory activity of human IgA antibodies and their Fab alpha fragments: Inhibition of IgG-mediated complement activation. *Eur. J. Immunol.* **19**, 2243–2249 (1989).
17. S. Fagarasan, G. Magri, A. Cerutti, "The mucosal immune system: Host-bacteria interaction and regulation of immunoglobulin A synthesis" in *Molecular Biology of B Cells*, F. W. Alt, T. Honjo, A. Radbruch, M. Reth, Eds. (Academic, New York, 2015), **vol. 60**, pp. 277–291.
18. R. Iversen *et al.*, Strong clonal relatedness between serum and gut IgA despite different plasma cell origins. *Cell Rep.* **20**, 2357–2367 (2017).
19. P. Brandtzaeg, H. Prydz, Direct evidence for an integrated function of J chain and secretory component in epithelial transport of immunoglobulins. *Nature* **311**, 71–73 (1984).
20. J. J. Bunker, A. Bendelac, IgA responses to microbiota. *Immunity* **49**, 211–224 (2018).
21. H. W. Schroeder, Jr, L. Cavacini, Structure and function of immunoglobulins. *J. Allergy Clin. Immunol.* **125**(Suppl 2), S41–S52 (2010).
22. V. Sørensen *et al.*, Effect of the IgM and IgA secretory tailpieces on polymerization and secretion of IgM and IgG. *J. Immunol.* **156**, 2858–2865 (1996).
23. S. Guenzi *et al.*, The efficiency of cysteine-mediated intracellular retention determines the differential fate of secretory IgA and IgM in B and plasma cells. *Eur. J. Immunol.* **24**, 2477–2482 (1994).
24. A. Bastian, H. Kratzin, K. Eckart, N. Hilschmann, Intra- and interchain disulfide bridges of the human J chain in secretory immunoglobulin A. *Biol. Chem. Hoppe Seyler* **373**, 1255–1263 (1992).
25. S. Frutiger, G. J. Hughes, N. Paquet, R. Lüthy, J. C. Jaton, Disulfide bond assignment in human J chain and its covalent pairing with immunoglobulin M. *Biochemistry* **31**, 12643–12647 (1992).
26. D. Pasalic *et al.*, A peptide extension dictates IgM assembly. *Proc. Natl. Acad. Sci. U.S.A.* **114**, E8575–E8584 (2017).
27. J. D. Atkin, R. J. Pleass, R. J. Owens, J. M. Woof, Mutagenesis of the human IgA1 heavy chain tailpiece that prevents dimer assembly. *J. Immunol.* **157**, 156–159 (1996).
28. E. van Anken *et al.*, Efficient IgM assembly and secretion require the plasma cell induced endoplasmic reticulum protein pERp1. *Proc. Natl. Acad. Sci. U.S.A.* **106**, 17019–17024 (2009).
29. H. Flach *et al.*, Mzb1 protein regulates calcium homeostasis, antibody secretion, and integrin activation in innate-like B cells. *Immunity* **33**, 723–735 (2010).
30. Y. Shimizu, L. Meunier, L. M. Hendershot, pERp1 is significantly up-regulated during plasma cell differentiation and contributes to the oxidative folding of immunoglobulin. *Proc. Natl. Acad. Sci. U.S.A.* **106**, 17013–17018 (2009).
31. M. Rosenbaum *et al.*, MZB1 is a GRP94 cochaperone that enables proper immunoglobulin heavy chain biosynthesis upon ER stress. *Genes Dev.* **28**, 1165–1178 (2014).
32. T. M. McIntyre, M. R. Kehry, C. M. Snapper, Novel in vitro model for high-rate IgA class switching. *J. Immunol.* **154**, 3156–3161 (1995).
33. A. J. Macpherson, Y. Köller, K. D. McCoy, The bilateral responsiveness between intestinal microbes and IgA. *Trends Immunol.* **36**, 460–470 (2015).
34. S. A. Ha *et al.*, Regulation of B1 cell migration by signals through Toll-like receptors. *J. Exp. Med.* **203**, 2541–2550 (2006).
35. T. Hisajima, Y. Kojima, A. Yamaguchi, R. C. Goris, K. Funakoshi, Morphological analysis of the relation between immunoglobulin A production in the small intestine and the enteric nervous system. *Neurosci. Lett.* **381**, 242–246 (2005).
36. J. F. Kearney, A. Radbruch, B. Liesegang, K. Rajewsky, A new mouse myeloma cell line that has lost immunoglobulin expression but permits the construction of antibody-secreting hybrid cell lines. *J. Immunol.* **123**, 1548–1550 (1979).
37. L. Hendershot, D. Bole, G. Köhler, J. F. Kearney, Assembly and secretion of heavy chains that do not associate posttranslationally with immunoglobulin heavy chain-binding protein. *J. Cell Biol.* **104**, 761–767 (1987).
38. I. G. Haas, M. Wabl, Immunoglobulin heavy chain binding protein. *Nature* **306**, 387–389 (1983).
39. A. J. Melnick, S. Aviel, Y. Argon, The endoplasmic reticulum stress protein GRP94, in addition to BiP, associates with unassembled immunoglobulin chains. *J. Biol. Chem.* **267**, 21303–21306 (1992).
40. V. Sørensen, V. Sundvold, T. E. Michaelsen, I. Sandlie, Polymerization of IgA and IgM: Roles of Cys309/Cys414 and the secretory tailpiece. *J. Immunol.* **162**, 3448–3455 (1999).
41. R. M. Parkhouse, Immunoglobulin a biosynthesis. Intracellular accumulation of 7 S subunits. *FEBS Lett.* **16**, 71–73 (1971).
42. A. Bargellesi, P. Periman, M. D. Scharff, Synthesis, assembly, and secretion of globulin by mouse myeloma cells. IV. Assembly of IgA. *J. Immunol.* **108**, 126–134 (1972).
43. Z. Moldoveanu, M. L. Egan, J. Mestecky, Cellular origins of human polymeric and monomeric IgA: Intracellular and secreted forms of IgA. *J. Immunol.* **133**, 3156–3162 (1984).
44. A. J. Macpherson, K. D. McCoy, F. E. Johansen, P. Brandtzaeg, The immune geography of IgA induction and function. *Mucosal Immunol.* **1**, 11–22 (2008).
45. J. M. Woof, M. W. Russell, Structure and function relationships in IgA. *Mucosal Immunol.* **4**, 590–597 (2011).
46. N. K. Surana, D. L. Kasper, Moving beyond microbiome-wide associations to causal microbe identification. *Nature* **552**, 244–247 (2017).
47. X. Song *et al.*, Growth factor FGF2 cooperates with interleukin-17 to repair intestinal epithelial damage. *Immunity* **43**, 488–501 (2015).
48. R. Zimmermann, Components and mechanisms of import, modification, folding, and assembly of immunoglobulins in the endoplasmic reticulum. *J. Clin. Immunol.* **36** (Suppl 1), 5–11 (2016).
49. L. Ellgaard, N. McCaul, A. Chatsisvili, I. Braakman, Co- and post-translational protein folding in the ER. *Traffic* **17**, 615–638 (2016).
50. M. Vanhove, Y. K. Usherwood, L. M. Hendershot, Unassembled Ig heavy chains do not cycle from BiP in vivo but require light chains to trigger their release. *Immunity* **15**, 105–114 (2001).
51. J. Mestecky, R. E. Schrohenloher, R. Kulhavy, G. P. Wright, M. Tomana, Site of J chain attachment to human polymeric IgA. *Proc. Natl. Acad. Sci. U.S.A.* **71**, 544–548 (1974).
52. B. A. Hendrickson *et al.*, Altered hepatic transport of immunoglobulin A in mice lacking the J chain. *J. Exp. Med.* **182**, 1905–1911 (1995).
53. V. Snoeck, I. R. Peters, E. Cox, The IgA system: A comparison of structure and function in different species. *Vet. Res.* **37**, 455–467 (2006).
54. W. R. Brown, T. M. Kloppel, The role of the liver in translocation of IgA into the gastrointestinal tract. *Immunol. Invest.* **18**, 269–285 (1989).
55. V. Andreani *et al.*, Cochaperone Mzb1 is a key effector of Blimp1 in plasma cell differentiation and β1-integrin function. *Proc. Natl. Acad. Sci. U.S.A.* **115**, E9630–E9639 (2018).
56. F. E. Johansen, C. S. Kaetzel, Regulation of the polymeric immunoglobulin receptor and IgA transport: New advances in environmental factors that stimulate pIgR expression and its role in mucosal immunity. *Mucosal Immunol.* **4**, 598–602 (2011).
57. L. Wang *et al.*, T regulatory cells and B cells cooperate to form a regulatory loop that maintains gut homeostasis and suppresses dextran sulfate sodium-induced colitis. *Mucosal Immunol.* **8**, 1297–1312 (2015).
58. A. T. Cao, S. Yao, B. Gong, C. O. Elson, Y. Cong, Th17 cells upregulate polymeric Ig receptor and intestinal IgA and contribute to intestinal homeostasis. *J. Immunol.* **189**, 4666–4673 (2012).
59. B. P. Ganesh, R. Klopfleisch, G. Loh, M. Blaut, Commensal *Akkermansia muciniphila* exacerbates gut inflammation in *Salmonella typhimurium*-infected gnotobiotic mice. *PLoS One* **8**, e74963 (2013).
60. M. A. Borton *et al.*, Chemical and pathogen-induced inflammation disrupt the murine intestinal microbiome. *Microbiome* **5**, 47 (2017).
61. N. W. Palm *et al.*, Immunoglobulin A coating identifies colitogenic bacteria in inflammatory bowel disease. *Cell* **158**, 1000–1010 (2014).
62. E. Elinav *et al.*, NLRP6 inflammasome regulates colonic microbial ecology and risk for colitis. *Cell* **145**, 745–757 (2011).
63. J. Downes, F. E. Dewhirst, A. C. Tanner, W. G. Wade, Description of *Alloprevotella rava* gen. nov., sp. nov., isolated from the human oral cavity, and reclassification of *Prevotella tannerae* Moore et al. 1994 as *Alloprevotella tannerae* gen. nov., comb. nov. *Int. J. Syst. Evol. Microbiol.* **63**, 1214–1218 (2013).
64. J. Liu *et al.*, Oral hydroxysafflor yellow A reduces obesity in mice by modulating the gut microbiota and serum metabolism. *Pharmacol. Res.* **134**, 40–50 (2018).
65. Y. Li *et al.*, EAF2 mediates germinal centre B-cell apoptosis to suppress excessive immune responses and prevent autoimmunity. *Nat. Commun.* **7**, 10836 (2016).
66. R. Ouchida *et al.*, Critical role of the IgM Fc receptor in IgM homeostasis, B-cell survival, and humoral immune responses. *Proc. Natl. Acad. Sci. U.S.A.* **109**, E2699–E2706 (2012).
67. J. Liu *et al.*, Efficient induction of Ig gene hypermutation in ex vivo-activated primary B cells. *J. Immunol.* **199**, 3023–3030 (2017).
68. T. A. Shih, M. Roederer, M. C. Nussenzweig, Role of antigen receptor affinity in T cell-independent antibody responses in vivo. *Nat. Immunol.* **3**, 399–406 (2002).
69. S. N. Murthy *et al.*, Treatment of dextran sulfate sodium-induced murine colitis by intracolonic cyclosporin. *Dig. Dis. Sci.* **38**, 1722–1734 (1993).